RESEARCH ARTICLE

The regular pattern and underlying mechanisms of seawater intrusion in the Modaomen channel in the Pearl River Estuary of China

Muzhen Yang[1] · Guoping Tang[1] · Tao Jiang[1] · Tao Chen[1] · Xiaohua Chen[1]

Abstract

In recent decades, the frequency and severity of inland river seawater intrusion has increased in the Pearl River Estuary (PRE) of China. Based on time series of water salinity data, river discharges, tides, and wind records for the period 2003–2015, this study aims to examine the regular pattern and underlying mechanisms of the seawater intrusion in the Modaomen channel of the PRE. Toward this end, the autocorrelation and spectral analysis are used to quantify the periodicity of runoff, tide, and water salinity and to infer the regular patterns of seawater intrusion. The Pearson correlation and the LMG metric are used to examine the effects of influencing factors on seawater intrusion. Results indicate that seawater intrusion in the Modaomen channel has distinct annual (369 days) and half-monthly (14.8 days) cycles, corresponding well with annual and half-monthly tidal cycles. Spatially, the frequency, severity, and periodicity of seawater intrusion decrease with increased landward distance away from the channel mouth. The prevention of seawater intrusion by incoming river flow becomes more remarkable as freshwater flows downstream. Shifts in wind speed and direction can strengthen or weaken seawater intrusion, depending on if wind is in the opposite or same direction of river flow. Further analysis using the LMG metric suggests that river discharge plays a dominant role in governing seawater intrusion. Overall, river discharges, tides, and wind are three major forces triggering the inland river seawater intrusion and account for, respectively, 46%, 15%, and 15% of the variation of water salinity in the Modaomen channel. The study is featured in not only identifying the major factors in driving seawater intrusion but also quantifying their relative contribution. Thus, the findings are important for water resources manager to predict and manage inland river seawater intrusion in the PRE of China.

Introduction

Inland river seawater intrusion along the coastal channels can be induced by various forces such as the rise and fall of tides (Chen et al. 2019; Gong et al. 2018). Because seawater intrusion threatens the security and quality of water supply to surrounding regions (Cui et al. 2015; Franceschini and Signorini

✉ Guoping Tang
tanggp3@mail.sysu.edu.cn

✉ Tao Jiang
eesjt@mail.sysu.edu.cn

[1] School of Geography and Planning, Department of Physical Geography, Resources and Environment, Sun Yat-sen University, Guangzhou 510275, China

2016; Gong and Shen 2011), it has long troubled people worldwide and attracted researchers' attention for decades (Javadi et al. 2013; Werner and Gallagher 2006; Shi and Jiao 2014; Tang et al. 2020). In recent decades, climate change–associated sea level rise intensifies inland river seawater intrusion and augments its detrimental effects on coastal aquifers (Abd-Elhamid and Javadi 2011; Tamez-Meléndez et al. 2016; van den Brink et al. 2019; Torres-Martinez et al. 2019; Mora et al. 2020) and channels (Chen et al. 2016; Yuan et al. 2015). In addition, anthropogenic activities such as rapid urbanization and increasing channel water intakes for domestic and industrial uses in coastal areas (Cui et al. 2007; Yuan and Zhu 2015; Zhang et al. 2017) deteriorate freshwater resources and the condition of vegetation and soil in invaded areas (Garcia et al. 2010). This in return leads to a greater threat to the socioeconomic development of coastal communities (Gain et al. 2012; He et al. 2019).

The driving forces of seawater intrusion can involve natural and anthropogenic factors (Shaha et al. 2013). Decrease in river discharge, increase in tidal level, shifts in wind direction and speed (Chen et al. 2019; Gong et al. 2018), rise in sea level (Hong et al. 2020), and decrease in regional rainfall (Adrian et al., 2009; Wu et al. 2013) are general natural forces that trigger inland river seawater intrusion (Adrian et al., 2009; Lu and Du 2006; Liu et al. 2010). Anthropogenic activities such as groundwater overexploitation, riverbed undercutting due to sand dredging (Li et al., 2019), and the storage of river water by reservoirs or the diversion of river water by aqueducts for other uses in upper reaches can trigger seawater intrusion in coastal areas due to decreasing incoming river flow (Bithin et al., 2009; Fang 2013). In fact, these factors interact and jointly affect seawater intrusion in coastal channels. Thus, knowledge of major factors and their roles in governing seawater intrusion is important for securing water supply to ecosystems and social communities in the coastal region (Ghafouri and Parsa, 2003; Han et al. 2010; Song et al. 2014; Xu et al. 2019).

In recent decades, inland river seawater intrusion in the Pearl River Estuary (PRE) of China tends to last longer and bring severer negative effects on the region (Hou and Su 2009; Liu et al. 2019a, b, c). For example, a super-large seawater intrusion occurring in the end of 2005 swept across the region and endangered water supply to nearby cities such as Zhongshan, Zhuhai, and Macau. As a result, the local governments have to seek water from other regions to copy with water shortage (Cui et al. 2015; Liu et al. 2019a), which affected more than 1.5 million population in the Pearl River Delta region (Hou and Su 2009; You et al. 2009). Even in 2016, a high flow year, the effect of seawater intrusion on Zhongshan city lasted for 6 months (Liu 2020). In addition, inland river seawater intrusion in the PRE tends to intrude farther and occurs earlier on an annual time basis (Kong et al. 2011; Liu et al. 2016). Therefore, understanding the features of seawater intrusion becomes essential for managing the seawater intrusion in the PRE.

Many efforts were made to examine the regular pattern and driving forces of seawater intrusion in the PRE of China, including theoretical research, quantitative analysis, numerical modeling, laboratory and field experiments, as well as engineering project regulation (Bao et al. 2009; Gong and Shen 2011; Hu et al. 2019; Jia et al. 2006; Lei and Jiu, 2014; Lin et al. 2019; Tang et al. 2020). Hu and Mao (2012) found that the regular cycle of chlorine content in the Modaomen channel was about 15 days, and the variation of salinity in each cycle was subject to river runoff. Song et al. (2014) claimed that seawater intrusion in PRE was mainly driven by shifts in runoff and tides. Zou et al. (2019) have investigated the effect of riverbed degradation on seawater intrusion in the Modaomen estuary, and they found that riverbed degradation results in an obvious increase of salinity at the bottom layer.

Other studies investigated the effects of river discharge, tides, winds, and sea level rise on seawater intrusion based on daily observation data (Lin et al. 2019; Wang et al. 2020). Nevertheless, a comprehensive study on the features and an exploring of quantifying driving forces of seawater intrusion in the PRE are still limited.

This study aims to analyze the pattern of seawater intrusion in the PRE of China and to quantify the roles of major factors in affecting seawater intrusion in the region. To achieve the goals, we selected the Modaomen channel in the PRE as the study site. Time series of water salinity from four water pumping stations in the channel, river discharges, and tidal levels from the Sanzaodao station, as well as wind speed for the 2003–2015 period, were collected and used for this study. Statistical methods such as linear and multiple regression analysis, autocorrelation, and spectral analysis were conducted to examine the features and underlying driving forces of seawater intrusion in the Modaomen channel. The paper is organized as follows: "Method and data" section describes the method and data used to analyze the seawater intrusion pattern and mechanism in the PRE of China. "Results" section describes the analytical results. "Discussion" section discusses the reasonability of our findings through comparison with previous studies and the underlying mechanisms for seawater intrusion in PRE of China. Finally, "Conclusions" section presents our conclusions.

Method and data

Study site

The Modaomen channel located in the PRE of China is the main stream of Xijiang and Beijiang River. As the primary channel of the eight outlets in the PRE (Song et al. 2014), it transports a significant amount of fresh water and sand (Chen et al. 2009) from the aforementioned two rivers into the coastal sea. In addition, it supplies water to nearby cities like Zhuhai and Macao. In recent decades, natural and anthropogenic factors have increased the frequency and severity of inland river seawater intrusion in PRE (Liu et al. 2018), which threats the socioeconomic development in the region. Because of its representativeness in the PRE and the availability of data records, the Modaomen channel was an ideal platform to analyze the patterns and driving forces of seawater intrusion in the PRE of China. Technically, the procedures of our analysis consist of four steps: (i) collecting data of water salinity, tides, river discharge, and wind speed; (ii) processing missing data; (iii) analyzing the pattern of seawater intrusion via autocorrelation and spectral analysis; and (iv) examining the underlying driving forces of seawater intrusion. The specific methods are described below.

Data and processing

Time series of water salinity for the period 2003–2015 were collected from Guadingjiao, Guangchang, Pinggang, and Zhuzhoutou water pumping stations (Table 1 and Fig. 1). The study focused on the 2003–2015 period largely because of the data missing and unavailable issues for other periods. Even for the 2003–2015 period, water salinities from the Guangchang and Pinggang stations are mainly at the daily step for the dry seasons of 2003–2008 and at the hourly step for the period of January 2010 to August 2015. For Zhuzhoutou station, daily water salinities span from February 2011 to August 2015. For these periods, the percentage of missing data in each year is less than 2% out of the total number of days in the calendar year. As for the missing data in a station, we used the interpolated values from the nearest station: firstly, the nonlinear least square method was used to build the functional relationship of water salinities between two neighboring stations; then, the derived function was used to fit daily missing values. We cross validated the interpolated values using observed corresponding data and found that differences (%) are mostly below 5%. For hourly water salinity data, the measured salinities from 1 to 24 o'clock were averaged to obtain daily salinity of that day.

We counted the number of annual seawater intrusions at each station if the daily water's salinity at a station exceeds 250 mg/l, and the duration of seawater intrusion is calculated from the day when water salinity rises beyond 250 mg/l to the day when it drops below 250 mg/l (The 250 mg/l isohaline is the recommended salinity threshold value of river water for drinking purposes according to the National Hygienic Standard for Drinking Water (GB 5749-2006) in China [Yuan et al. 2015].). Other data collected for this study include river discharges measured at the Makou and Sanshui station, observed daily high, low and mean tides (the average of highest and lowest tides) from the Sandzaodao station, and wind speeds from the Domen weather station. These data are also at daily step and match the temporal resolution of water salinity data.

Analytical methods

The autocorrelation and spectral analyses are used to analyze the periodicity of runoff, tide, and water salinity and to infer the regular patterns of seawater intrusion. They are also used to quantify the relationships of water salinity to the variation of tides, river discharges, and wind speed, respectively. The Pearson correlation coefficient is used to analyze the relationship between two variables and expressed as follows:

$$\rho_{XY} = \frac{\mathrm{Cov}(X, Y)}{\sqrt{D(X)}\ \sqrt{D(Y)}} = \frac{E((X-EX)(Y-EY))}{\sqrt{D(X)}\ \sqrt{D(Y)}} \quad (1)$$

where E is the mathematical expectation; D is variance; $E\{[X - E(X)][Y - E(Y)]\}$ is the covariance of X and Y and denoted as Cov (X, Y). ρ_{xy} ranges from −1 to 1. The greater the absolute value of ρ_{xy} is, the stronger the relationship between two variables is.

Furthermore, the proposed metric by Lindeman, Merenda, and Gold (LMG) relative importance metric (Grömping 2006) was used to evaluate the contribution of major driving forces to changes in water's salinity. In regression analysis, the R^2 coefficient is used to explain the proportion of the variation of a dependent variable that can be explained by the variation of independent variables. LMG metric decomposes the contribution of each independent variable to R^2, ensuring that the contribution of each independent variable is positive and that their sum is equal to R^2 (Kruskal 1987). Therefore, LMG is

Table 1 List of daily water salinity data and related data missing in this study

Year	Guangchang	Pinggang	Zhuzhoutou	Guadingjiao
2003	No[†]	No	—	No
2004	5.1–9.30[‡]	5.1–9.30	—	5.1–9.30
2005	4.1–9.17	4.1–9.17	—	4.1–9.17, & 10.11–12.31
2006	4.1–9.16	4.1–9.16	—	4.1–9.16
2007	3.1–10.15	3.1–10.15	—	3.1–10.15
2008	3.1–12.31	3.1–12.31	—	3.1–12.31
2009	3.1–9.90	3.1–9.90	—	No
2010	No	No	No	No
2011	No	No	1.1–1.31 & 7.15–8.25	No
2012	5.1–8.31	No	No	No
2013	8.14–10.9	No	No	No
2014	No	No	No	No
2015	8.27–12.31	8.27–12.31	8.27–12.31	No

[†] denotes there is no data missing for this given year; [‡] means that there is no daily salinity data for the specified period in this given year: "—" means no data available for the whole year

Fig. 1 The Modaomen channel
and surrounding topography in
the Pearl River Delta and Estuary
of China
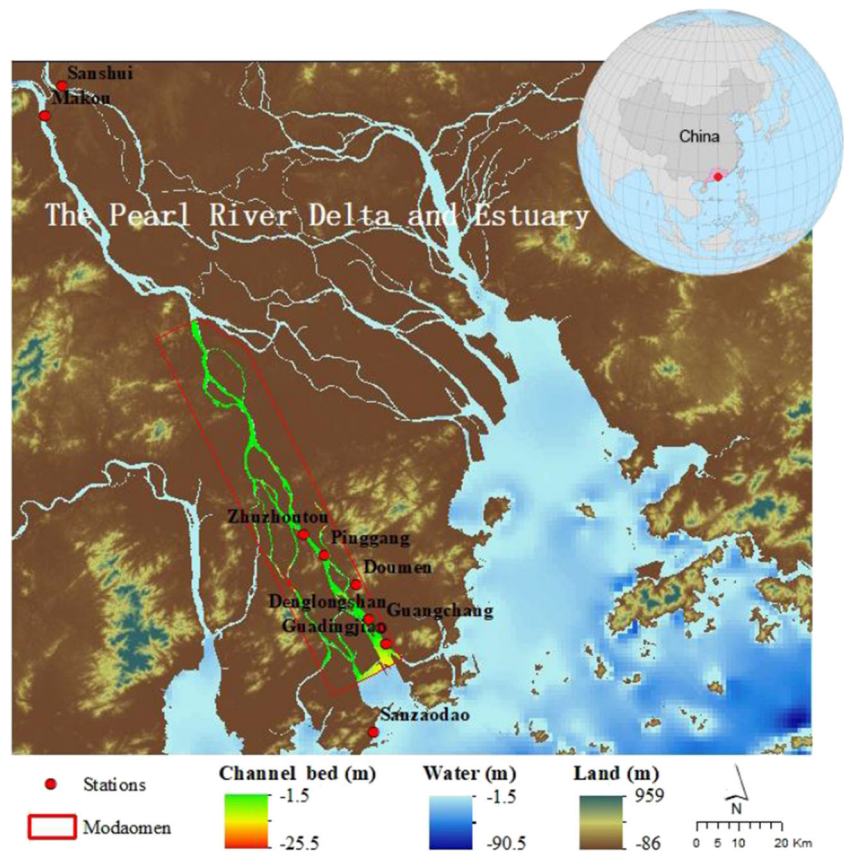
widely used to measure the relative importance of independent variables to a dependable variable (Johnson and Lebreton 2004). The calculation of LMG is expressed as follows:

$$LMG(i) = \frac{1}{p!} \sum_{r\_permutation} s\_var(i|S_i(r)) \qquad (2)$$

Equation (2) represents the calculation of the LMG value of x_i; $r\_permutation$ represents that the independent variable enters the equation in the order from 1 to p; $S_i(r)$ represents the set of existing independent variables before x_i enters the equation; $s\_var(i|S_i(r))$ refers to the change in R^2 caused by x_i when there is already a set of $S_i(r)$ variables in the model. For all the independent variables entered into the r arrangement of the equation, the variation of R^2 caused by x_i entering the equation was averaged, that is, the LMG value of x_i (Sun et al. 2012; Tang et al., 2019).

Results

The variations of seawater intrusion in the study period

Figure 2 a shows the variations of water salinity at the Guadingjiao, Guangchang, and Pinggang stations in 2003,

respectively. From Fig. 2, seawater intrusions at each station mainly occur from October to April of the next year. However, as the distance of the station from the sea increases landward, the number of seawater intrusions varies distinctly. The farther the station is away from the sea, the less the seawater intrusion reaches the station, and vice versa (Fig. 2c). For example, because the Pinggang station is located farther away from the sea than the Guangchang station, the seawater intrusions at the Pinggang station, on average, lasted about 7 days, whereas it lasted 31 days at the Guangchang station in December of 2003. Besides, the extent of water salinity exceeding 250 mg/l varied remarkably across stations. For seawater intrusion occurring at the same time, the closer the station is to the sea, the higher the water salinity is, and vice versa. For example, the highest salinity at the Guadingjiao, Guangchang, and Pinggang stations was 7834.6, 5443.7, and 1341.5 mg/l, respectively, in December of 2003 (Fig. 2a).

Figure 2b shows the variation of average daily salinity for the period 2010–2015. The occurrence and frequency of seawater intrusion at multi-annual scale are similar to that in 2003. The Pinggang and Zhuzhoutou stations are neighboring stations and both are located farther away from the sea than the Guangchang station. As a result, the magnitudes and variations of seawater intrusions between the two stations are relatively consistent, mainly occurring from December to February of the next year (Fig. 2b). In contrast, because the

Fig. 2 **a** The variation of daily water salinity at the Guadingjiao, Guangchang, and Pinggang station in 2003. The 2003 seawater intrusion was used here because the seawater intrusion was severe and typical in history; **b** the variation of average water salinity at the Guangchang, Pinggang, and Zhuzhoutou station for the 2010–2015 period. Due to data missing issue, water salinities for the period of 2004–2009 were not shown here; **c** the total numbers that the seawater intrusion occurred on a calendar day, respectively, during the 2010–2015 period at the Guangchang, Pinggang, and Zhuzhoutou station. The red lines in (**a**) and (**b**) represent water salinity at the 250 mg/l level
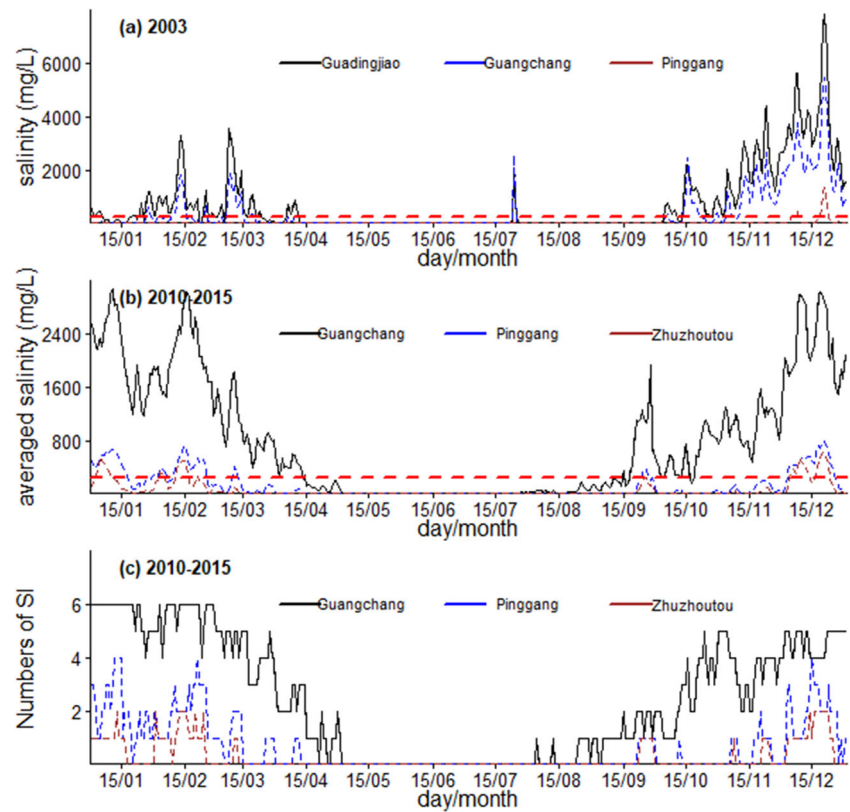
Guangchang station is located closer to the sea, the average water salinity during seawater intrusions is much greater than at the other two stations. The intrusion also begins earlier and ends later at the Guangchang station, starting from mid-August to the end of April of next year, while it is from mid-September to mid-April of the next year at the other two stations (Fig. 2b).

Figure 3 shows the variation of the number of days and hours that the water salinity at a station exceeds 250 mg/l during the study period. At the Pinggang station, the number of days with water salinity exceeding 250 gm/l increased from 2003 to 2008 and decreased from 2010 to 2015. Similarly, the number of hours with water salinity exceeding 250 mg/l showed a declining trend from 2010 to 2015 at the Guangchang station. In addition, the changing trend varies among stations. For example, compared to 2012, the number of hours that the water salinity exceeding 250 mg/l decreased slightly at the Guangchang station in 2013, whereas it decreased significantly at the Pinggang and Zhuzhoutou stations (Fig. 3b).

The periodicity of seawater intrusions in the Modaomen channel

Figure 4 shows the results of the spectral analysis on time series of daily water salinity at the Guangchang, Pinggang, and Zhuzhoutou stations, respectively. The seawater

intrusions at these stations have a distinct annual (about 369 days) and a half-monthly (about 14.76 days) cycle. Spatially, the closer the station is to the sea, the more significant the annual cycle is. For example, the annual cycle of seawater intrusion is more remarkable at the Guangchang station than at the Pinggang station. The differences in autocorrelation coefficients for monthly average salinity between the two stations prove that the closer the station is to the sea, the more significant the periodicity of the water salinity is. In contrast,
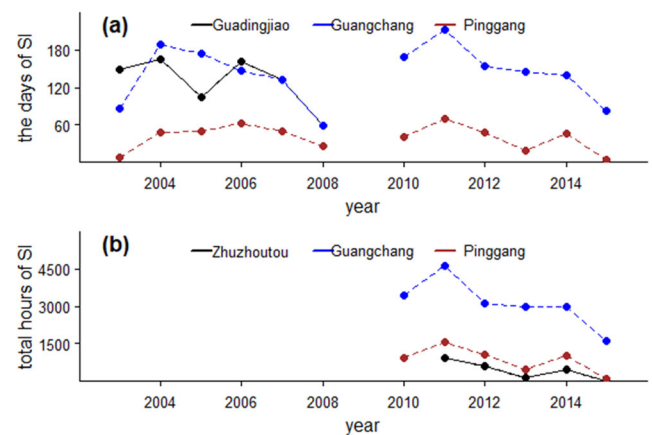
Fig. 3 **a** The days of seawater intrusions (SI) during the 2003–2015 period at the Guadingjiao, Guangchang, and Pinggang station; **b** the total hours of SI at the Zhuzhoutou, Guangchang, and Pinggang station during the 2010–2015 period. Due to data missing, no statistics are available for some years
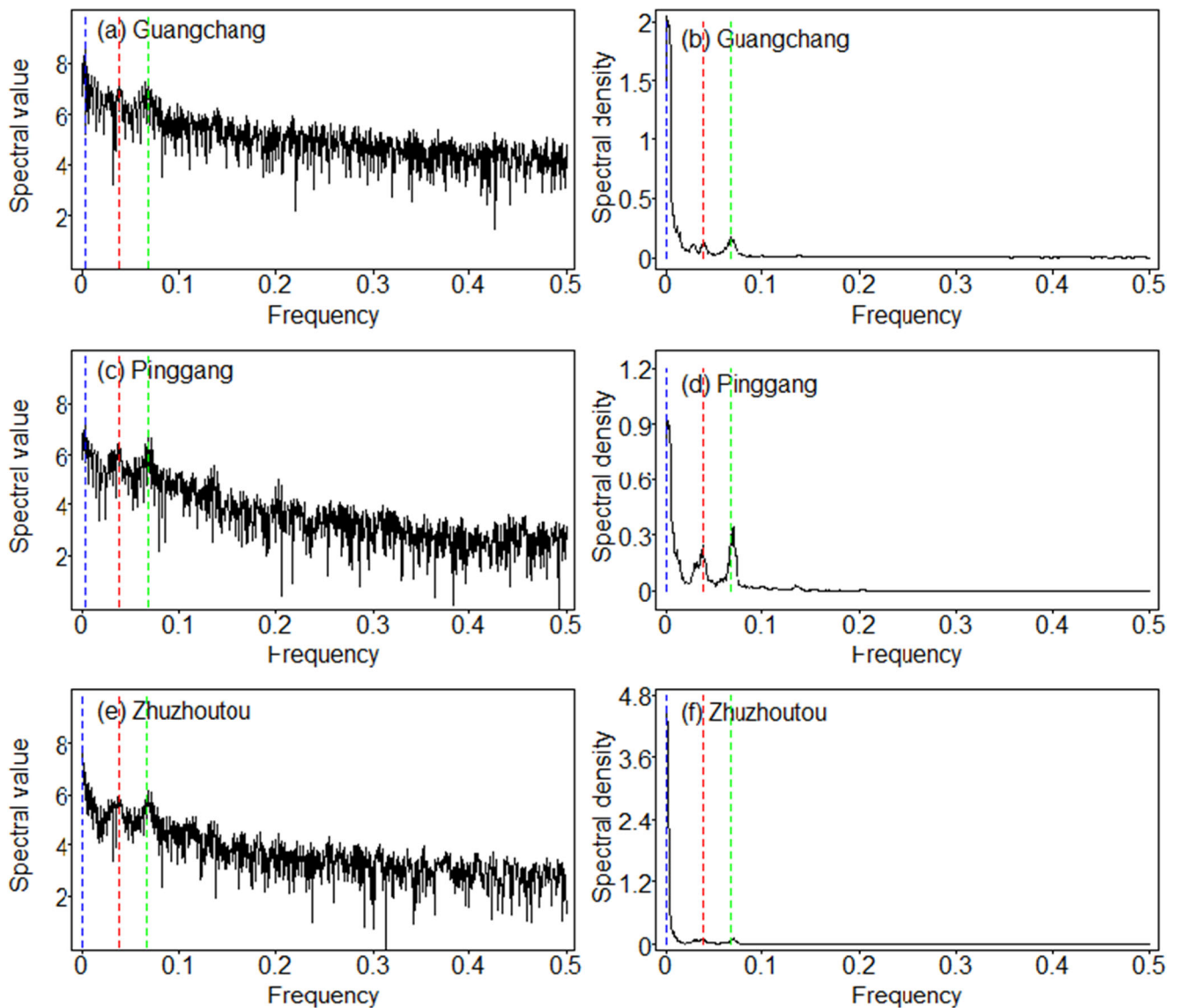
Fig. 4 Spectral analysis on time series of daily salinity data for the period of 2010–2015 observed at **a** Guangchang, **b** Pinggang, and **c** Zhuzhoutou station. Dashed blue, red, and green line represents that the water salinity has annual, monthly, and half-monthly cycles.

the half-monthly cycle (14.76 days) is more obvious at the Pinggang than that at the Guangchang station (lower density in Fig. 3b vs. higher density in Fig. 3d). For the Zhuzhoutou station, the annual cycle of water salinity is more notable than at Pinggang station, whereas the half-monthly cycle is not as distinct as at the other two stations (Fig. 3b, d, and f).

Figure 5 shows the mean and maximum salinities of water as well as the duration of seawater intrusion among the three stations are significantly and positively correlated with each other, respectively. If the maximum salinity of water increases by 1 mg/l at Guangchang, Pinggang, and Zhuzhoutou stations, the average water salinity will increase by 0.37, 0.45, and 0.47 mg/l, respectively. Similarly, the duration of seawater intrusion will increase by 0.05, 0.09, and 0.10 h (Fig. 5), respectively. Spatially, the increasing rate (suggested by the slopes in

Fig. 5) of mean water salinity as the maximum water salinity increases tends to be greater at a station if it is located farther away from the sea. This situation is reversed for the duration of seawater intrusion, the increasing rate of which tends to be smaller as the distance extends upstream from the channel mouth.

Effect of tides on inland river seawater intrusions

Figure 6 plots the results of the spectral analysis on time series of daily tide data at Sanzaodao station. The results indicate that the variations of high tides, low tides, and tide ranges are characterized by distinct half-monthly (about 14.76 days), monthly (about 27.58 days), and annual (about 369.23 days)
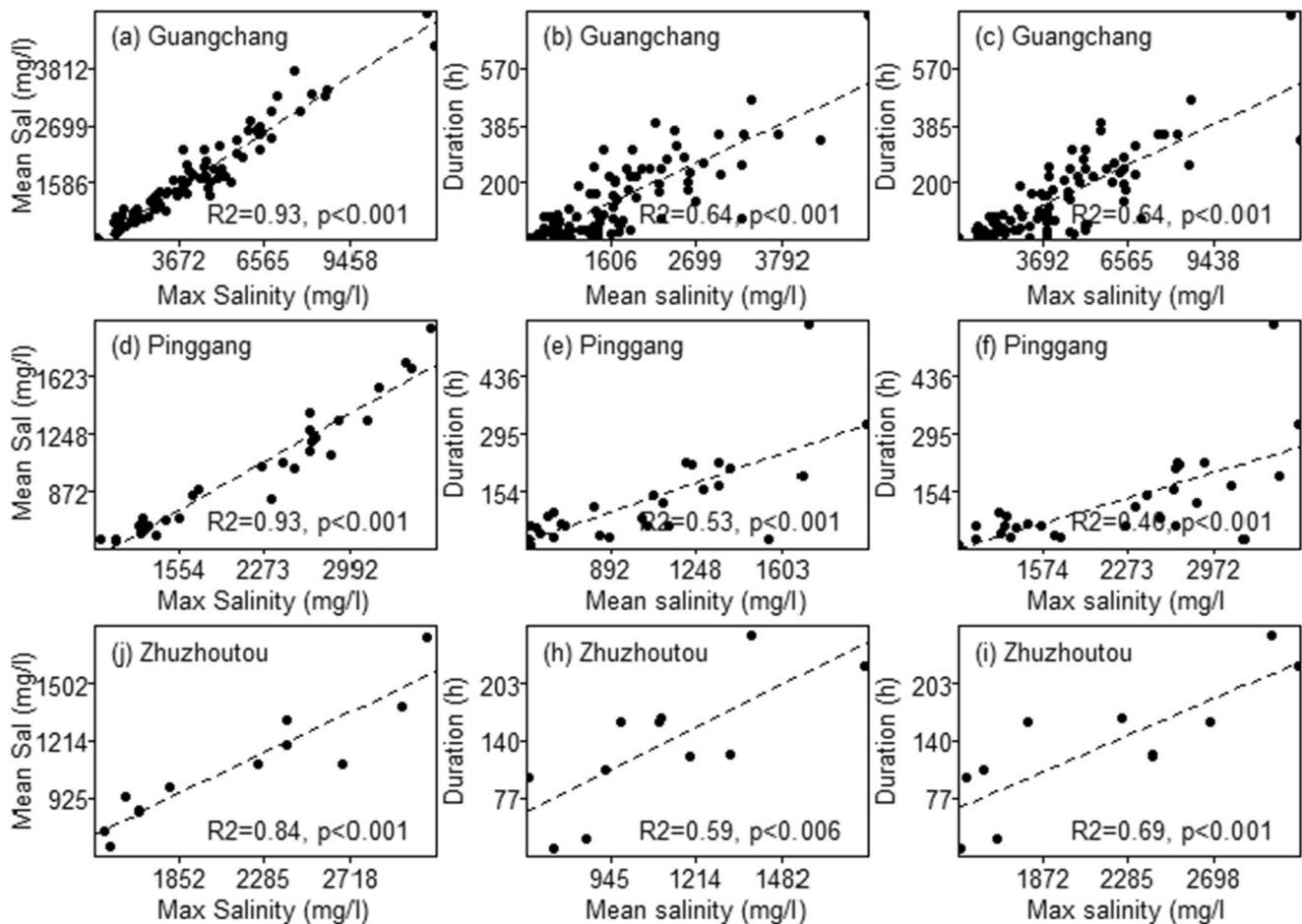
Fig. 5 The inter-relationships among maximum salinity, average salinity, and the duration of water salinity exceeding 250 mg/l during the 2010–2015 period at **a–b** Guangchang, **c–d** Pinggang, and **e–f** Zhuzhoutou station

cycle, respectively. Comparatively, the annual cycle is more remarkable than the half-monthly and monthly cycles.

Figure 7 presents the relationship of the autocorrelation coefficients of high tide, low tide, and tidal range at the Sanzaodao station with those of water salinities at Guangchang, Pinggang, and Zhuzhoutou station, respectively (Fig. 7). The results indicate that the periodicity of water salinity at the three stations is closely related to that of high and low tides. Compared to high and low tides, there is a hyperbolic relationship between tide ranges and water salinities at the three stations, and such a relationship is symmetric against the fitted regression line (Fig. 7c, f, i), suggesting that the water salinity at the three stations can either increase or decrease as tide range increases. Overall, the correlation between water salinity and low tides is highest. The closer a station is to the sea, the higher the correlation between water salinity and low tides is, indicating that the tidal occurrence is a major factor inducing inland river seawater intrusion.

Further analysis indicated that the peak salinity of water follows the occurrence of high tide. Figure 8 shows the variation of maximum water salinity and corresponding tidal height for the seawater intrusion with the longest duration

occurred at the Pinggang station. From the figure, the maximum water salinity was positively correlated with high tide. The correlation coefficient between maximum water salinity and high tide is 0.16. However, if the sequence of water salinity is moved forward by 4 h, the correlation coefficient increases to 0.41, suggesting that the effects of high tides on water salinity in the Modaomen channel were lagged by about 4 h.

Effects of river discharges on inland river seawater intrusion

Figure 9 shows the correlation between the river discharges and the water salinity at the Guangchang, Pinggang, and Zhuzhoutou stations. The results suggest that the water salinity at all stations was significantly and negatively correlated with incoming river discharges, respectively. If river discharge increases by 1000 m^3/s per day, the water salinity will decrease by 163 mg/l, 26 mg/l, and 14 mg/l, respectively, at the three stations. Also, the closer the station is to the sea, the stronger the correlation is. For instance, the correlation coefficients between monthly water salinity and discharge at the
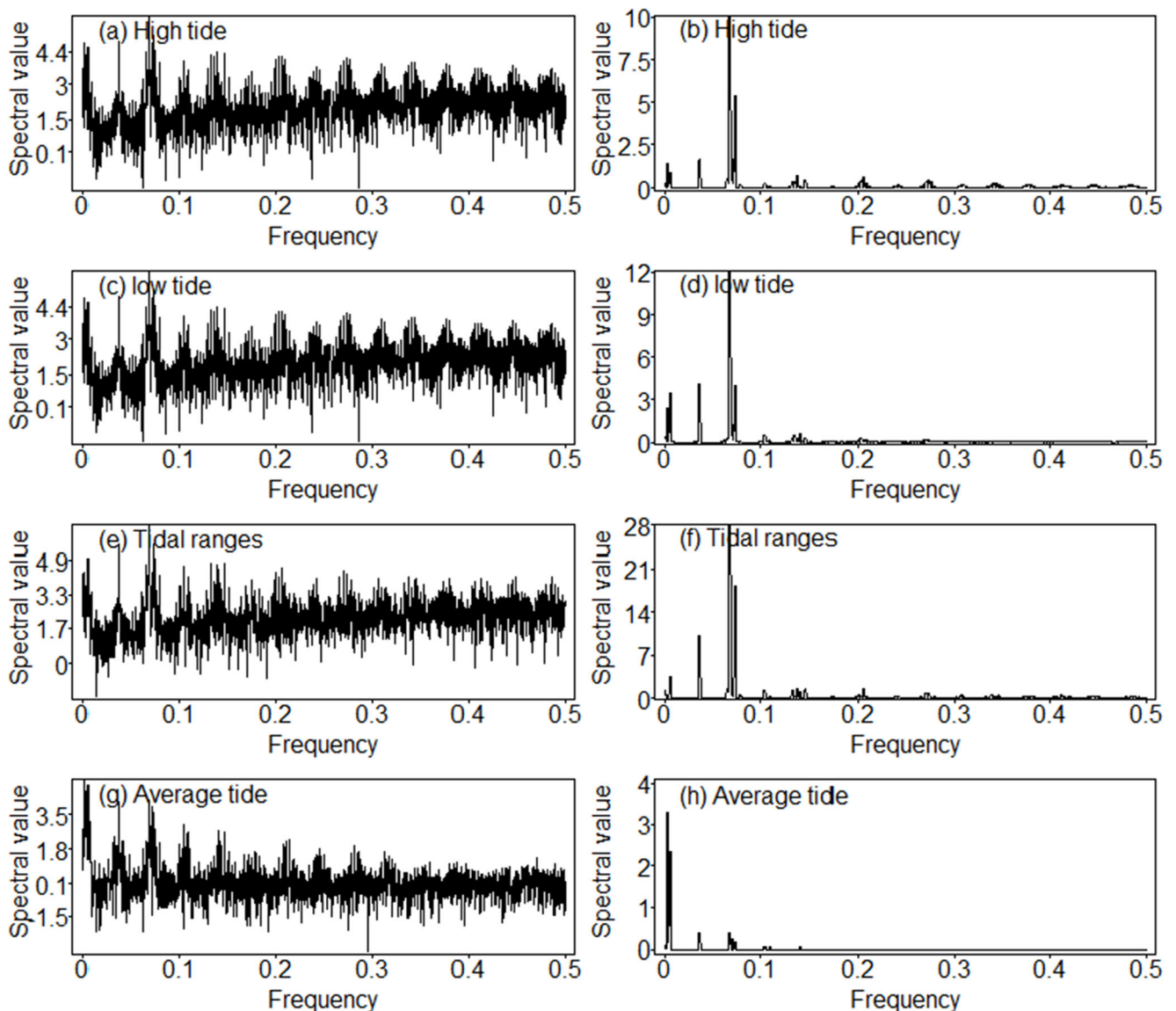
Fig. 6 The results of spectral analysis on time series of **a–b** high tides, **c–d** low tides, **e–f** tidal ranges (i.e., differences between high and low tides), and **g–h** average tides for the period of 2010–2015 observed at the Sanzaodao station

Guangchang, Pinggang, and Zhuzhoutou stations are −0.63, −0.46, and −0.40, respectively.

Further analysis indicates that the periodicity of river discharge was highly consistent with that of water salinity (Fig. 9d, e, and f), implying that the amount of river discharge is one of the main factors affecting seawater intrusion in the Modaomen channel. Additionally, the strength of the correlation (suggested by the R-squared values in Fig. 9d, e, and f) between the periodicity of river discharge and that of salinity increases as the distance of station away from the channel mouth increases landward, suggesting that the influence of river discharge on water salinity decreases with the increased landward distance away from the sea. In addition, the influence of discharge on water salinity in the dry season differs from that in the wet season. In specific, the strength of the correlation between discharge and water salinity in the wet season (from April to October) is smaller than in the dry season (from November to January of the next year), indicating that river discharge in the dry season has greater impacts on water salinity than that in the wet season.

Effects of wind on inland river seawater intrusions

Figure 10 shows the relationships between the water salinity at the Pinggang and Guangchang stations with mean, maximum, and extreme wind speed measured at the Domen weather station during 2011–2012, respectively. The results indicate that the water salinity during seawater intrusions at the Guangchang station was positively correlated with mean wind speed ($R^2=0.18$, $p < 0.001$), maximum wind speed ($R^2=0.09$,
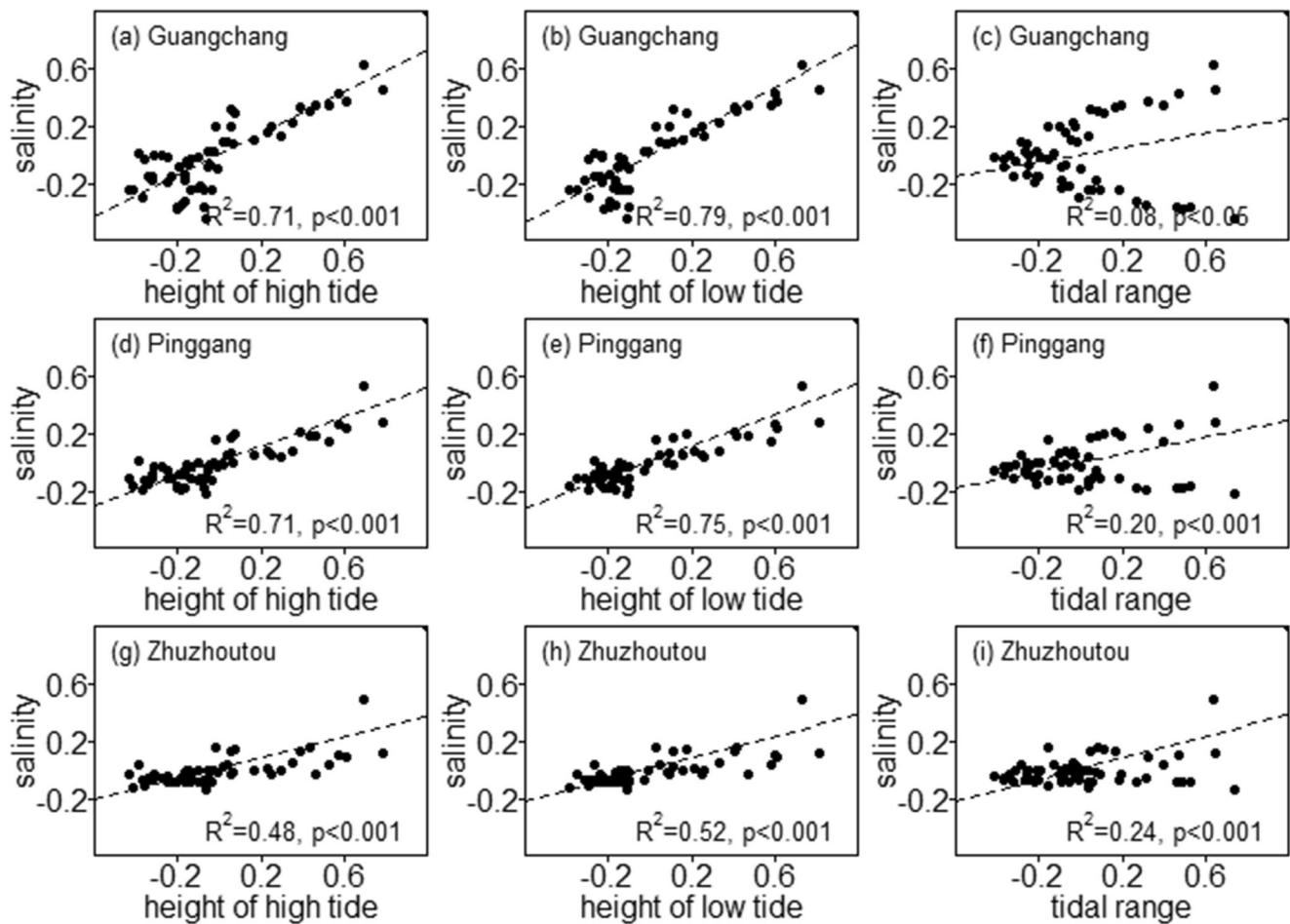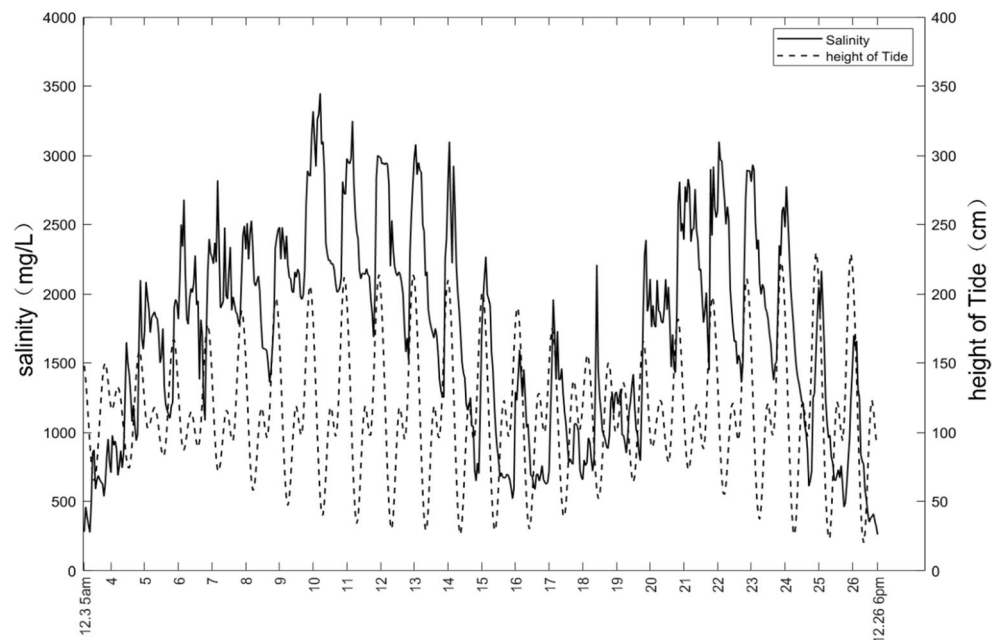
Fig. 7 The relationship between the autocorrelation coefficients for time series of water salinities and high tides, low tides, as well as tidal ranges at **a**–**c** Guangchang, **d**–**f** Pinggang, and **g**–**i** Zhuzhoutou station. Data shown here are for the period of 2010 to 2015

Fig. 8 Time series analysis of daily maximum water salinities at the Pinggang station and the corresponding tidal height at the Denglongshan station from 5 AM of December 3rd to 18 PM of December 26th, 2011
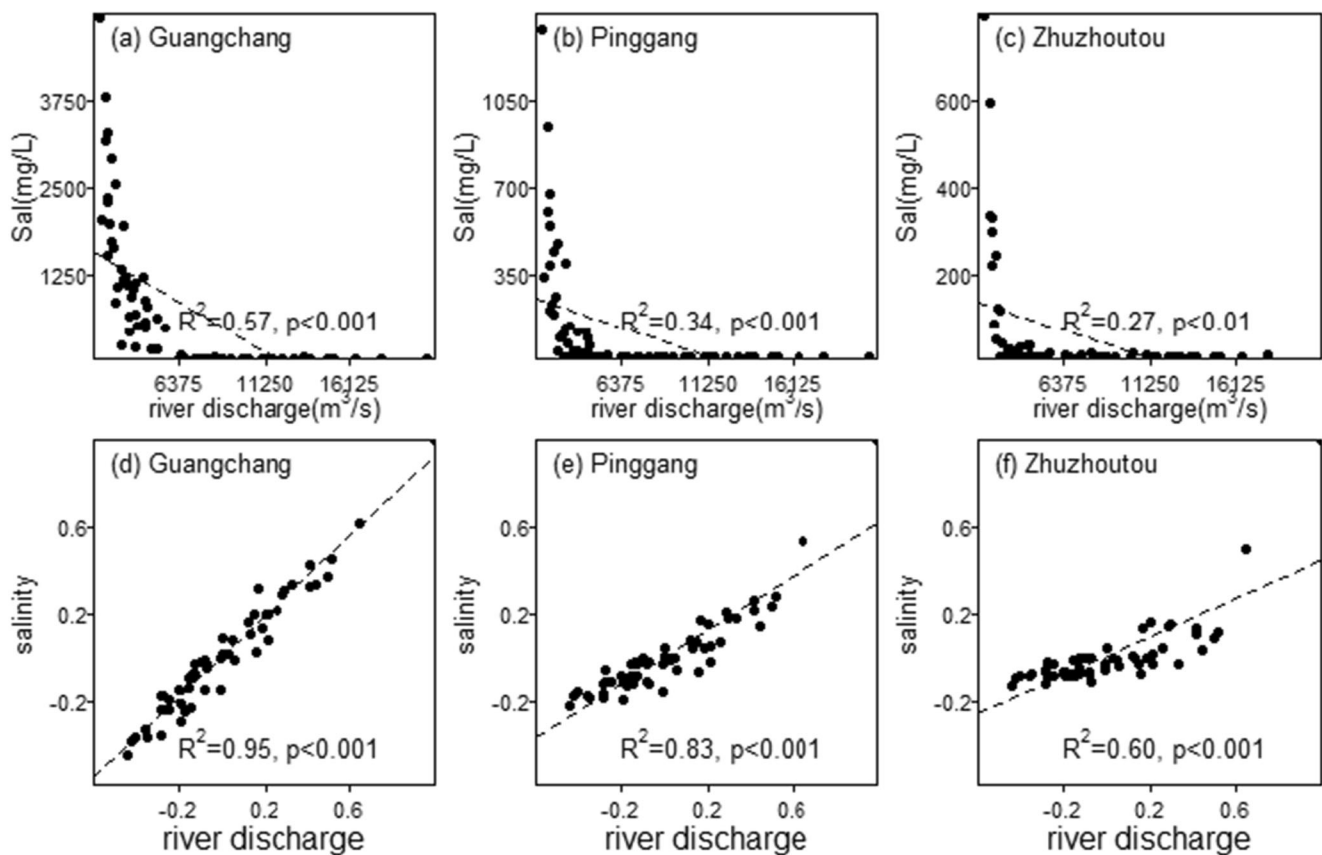
Fig. 9 The relationship between river discharge and water salinity as well as between the autocorrelation coefficients derived from time series of river discharges and water salinities for the period of 2010–2015 at **a**, **d** Guangchang, **b**, **e** Pinggang, and **c**, **f** Zhuzhoutou station, respectively.

For panel a, b, and c, the water's salinity does not vary remarkably during the wet season when river flow is approximately greater than 5000 $m^3/$ day

p<0.02), and extreme wind speed (R^2=0.10, p<0.02). At the Pinggang station, however, the water salinity is only significantly correlated with mean wind speed other than with the maximum and extreme wind speed (p>0.26), largely because the Pinggang station is located farther away from the sea. The region around the Modaomen channel prevails northward and northeastward wind (95%). Because the northward and northeastward wind is opposite to the direction of river flow (generally from northwest to southeast) but in line with the direction of seawater intrusion, the strengthening of northward and northwestward wind is conducive to inland river seawater intrusion.

Relative contribution of driving factors to seawater intrusion

Table 2 shows the results of the relative contribution of river discharges, tides, and wind speed to the water salinity in the Modaomen channel. From Table 2, river discharge, high tides, and wind speed are three main factors responsible for seawater intrusion in the Modaomen channel and jointly explain 79.4% of the variation of water salinity at the Guangchang station. In more detail, for a daily seawater intrusion at a station, changes

in river discharges on the previous and current day are negatively correlated with water salinity at the station and both jointly account for 58% of the 79.4% variation in water salinity. In contrast, the interaction of river discharge with tide and wind is positively correlated with water salinity, and they explain respectively 19% of the 79.4% variation of water salinity at the Guangchang station.

Discussion

The regular pattern of seawater intrusion in recent decades

Inland river seawater intrusion in the Modaomen channel has a distinct annual cycle, and this cycle corresponds well with the seasonality of wet and dry season, indicating that the upstream river flow plays an important role in inducing seawater intrusion in the Channel. Because river discharge is relatively low during the dry period of October to March of the next year, the likelihood of seawater intrusion is high. In contrast, because river discharge is high during the wet period of April to September, the likelihood of seawater intrusion is low (Cui
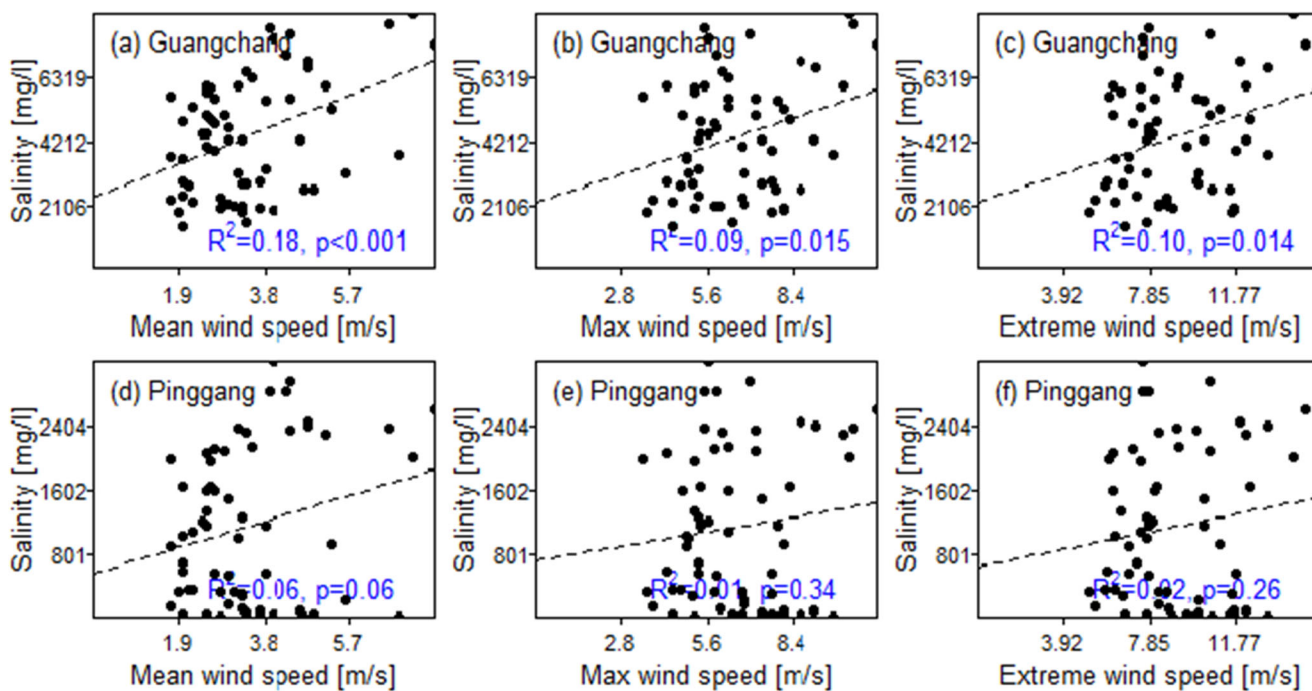
Fig. 10 The relationship of daily water salinity to average, maximum, and minimum wind speed at **a**–**c** Guangchang and **d**–**f** Pinggang station during extreme seawater intrusion in the period of 2011–2012

et al. 2015; Gong and Shen 2011). In addition, the cycle of water salinity corresponds also well to the cycle of tides as suggested in Bao et al. (2009), suggesting that the rise and fall of sea level also play an important role in triggering the seawater intrusion. Spatially, because river discharge suppresses seawater intrusion and the tidal forces attenuates as the tidal waves move upstream, the frequency and severity of seawater intrusion experienced at a station decrease with the increased landward distance away from the channel mouth.

Our results suggest that the severity of water salinity at a station may not reflect the duration of seawater intrusion at that station. This is understandable because the duration of seawater intrusion is defined as the length of time when water salinity exceeds 250 mg/l. When the tidal forces and upstream river

discharges keep relatively stable for a long time, the duration of seawater intrusion at a station can last long. Differences also exist in the frequency of seawater intrusion among different stations (Fig. 3). This may due to the effects of interaction among river discharges, tides, and wind on seawater intrusion in the channel. For stations closer to the sea, the tidal forces are more likely to outbalance the suppression of river discharge, and thus the stations will experience more seawater intrusions. Besides, the release of freshwater from upstream reservoirs may lead to different trends in saltiness and duration of seawater intrusion along the channel (Cui et al. 2015; Gong et al. 2014). This could help explain the total hours and days of seawater intrusion with water salinity exceeding 250 mg/l tended to decrease slightly at most stations (Fig. 3).

Table 2 The relative importance analysis by LMG method

Factors	p<	Signs of correlation	Relative contribution (%)
Discharge of today	<0.001	-	28
Discharge of yesterday	<0.001	-	30
Wind speed × high tide[†]	<0.001	-	4
Discharge × high tide[†]	<0.001	+	19
Wind speed × discharge[†]	<0.001	+	19
PVM[‡]			79.4

[†] The interaction between the two variables; PVM[‡] is short for the proportion of variance of water salinity explained by the model: $Sa = \log(SF_{pre}) + \log(SF) + Wind \times Tide + Wind \times SF + Tide \times SF$, in which Sa refers to water salinity; SF_{pre} refers to river discharge on the previous day; SF, Wind, and Tide refer to river discharge, high tide, and wind speed on a given day, respectively.

Effects of tides on inland river seawater intrusions

Previous studies indicated that tides in the PRE are characterized by different periodicities, including half-month, monthly, and annual cycles, which are highly consistent with we observed in the Modaomen channel. For example, the tides in the PRE are characterized by major and minor tidal floods in half a month (Chen et al. 2014), agreed well with the half-monthly cycle of water salinities we observed in this study (Fig. 4). Moreover, the significant correlation between the periodicity of tides with that of water salinity at most stations indicates that the rise and fall of tides is one of the main factors affecting inland river seawater intrusion, especially in a dry season (Liu et al. 2014; Lu and Du 2006; Zhang et al. 2010).

The tidal dynamic controls the variation of water salinity along the channel when the seawater intrudes upstream. Because of the landward progress of tidal waves, the peak of seawater intrusion usually occurs after the appearance of spring tide (Cheng et al. 2012). In the shortage of freshwater, the levels of water salinity rise as the tidal forces increase because of their cumulative effects. This explains there exists a strong positive relationship between water salinity and high tides as we observed in this study (Fig. 7). Additionally, due to the time required for the tidal wave to invade landward and the attenuation of tidal forces as waves move upstream, the peak salinity of the water is lagged by several hours following high tides (Fig. 8). The symmetric distribution of plotted points against the slope line between tidal ranges and water salinities (Fig. 7c, e, and f) is because the fluctuation of sea levels can either strengthen or counteract the seawater intrusion.

Effects of river discharges on seawater intrusions

Previous studies (Lin et al. 2019; Liu et al. 2017; Twigt et al. 2009; Zhou et al. 2017) indicated that a decrease in river discharge can trigger inland river seawater intrusion in the Modaomen channel, consistent with what we found in this study. For example, runoff has been considered the main or even the decisive factor (Gong and Shen 2011) affecting seawater intrusions in the PRE. Once river inflow increases, freshwater will crowd out salty water under the condition of a certain volume of the river channel. As a result, the overall salinity of water in the channel decreases and the inland river seawater intrusion will be suppressed to some degree. Therefore, changes in river discharge directly affect the intensity of seawater intrusion in a year (Liu et al. 2017). This explains why the salinity of the water at the three stations is strongly and negatively correlated with river discharges (Fig. 9).

In recent years, the diversion of freshwater from reservoirs in upper reaches into the Pearl River has a remarkable suppression effect on seawater intrusion. Zhou et al. (2017) indicated that streamflow alteration has a more direct impact on salinity variation than sea level changes. From 2010 to 2015, the decreasing numbers of seawater intrusion in the Modaomen estuary were closely associated with the dispatching of water from reservoirs in upper reach areas (e.g., Cui et al. 2007). During some dry years, if reservoirs in the upper reaches cannot release enough water to the river, the seawater intrusion becomes more intense. It is why the seawater intrusion was extremely severe in the PRE in 2011 because the reservoirs in the upper reaches cannot divert sufficient fresh water into the river.

Effect of wind on inland river seawater intrusions

Our results indicate that wind speed has a strong relationship with the variation of water salinity on a daily basis, in accordance with previous studies showing that changes in wind speed and direction affect the occurrence and retroactivity of seawater intrusions in PRE (Chen et al. 2019; Gong et al. 2018; Kong et al., 2015; Liu et al. 2010). For example, the local wind can strengthen seawater intrusion by lowering the water level in the eastern part of the estuary and increasing the bottom landward flow (Gong et al. 2018). In addition, because wind can either push tidal waves upstream or freshwater downstream into the sea, it can accelerate or weaken the mixing of salt- and freshwater. Because the Modaomen channel prevails northward and northwestern wind, it is why wind speed was found to be positively correlated with water salinity (Table 2 and Fig. 10). Gao and Cai (2020) indicated that the north wind speed can even change the transport way of seawater intrusion in Modaomen estuary. However, the duration of wind speed is often short, and the wind direction is subject to change. The effects of wind on water salinity are mostly instantaneous, with little long-term interference. This explains there is no longer a significant relationship between wind speed and water salinity at a monthly time scale, indicating that wind is a minor factor affecting seawater intrusions at a long-term temporal scale.

The relative contribution of driving factors to seawater intrusions

Our results indicate that runoff accounts for 58% of the variation of water salinity in the Modaomen channel, indicating that river discharge is the dominant factor governing seawater intrusion in Modaomen channel, highly in accordance with previous studies (Chen et al. 2011; Lin et al. 2019), indicating that river discharges contribute 57% of the variance of seawater intrusion and play the most important role. Besides, we found that the relative contribution of tides is low by themselves, whereas the interactions among tides, wind, and discharge play an important role in triggering seawater intrusion, also consistent with Lin et al. (2019), suggesting that the effect of tidal ranges is negligible in the Modaomen channel.

However, when river discharge is low, tidal events will become the most important forces triggering the upwelling of seawater intrusion. Huang et al. (2017) indicated that tides are the main driving force for the occurrence of severe seawater intrusion in 2011.

The contribution of the interaction between wind and river discharge to the variation of water salinity is about 19%, agreeing well with Lin et al. (2019), suggesting that the effect of wind contributes 13% of the variance of seawater intrusion in the Modaomen channel. However, there exist strong spatial differences in terms of wind effects on inland river seawater intrusion (Gong et al. 2018), and changes in wind speed and direction can either exaggerate or weaken seawater intrusion as well as the length of intrusion in the Modaomen channel. The study region prevails northward and northwestward wind during the dry season, which pushes seawater upstream and thus contributes to seawater intrusion (Wang et al. 2012). Overall, our estimate of the overall contribution (79.4%) of river discharges, high tides, and the wind is also highly consistent with Lin et al. (2019), suggesting that a combination of river discharge, tidal range, and winds explains 71% of the variance of seawater intrusion in the Modaomen channel.

Conclusions

Inland river seawater intrusion in the PRE of China has become severer and poses a greater threat to environmental health and socioeconomic development in the region. The results of this study indicate that:

1) Seawater intrusions in the Modaomen channel mainly occur in the dry season from October to April of the next year. The frequency, severity, and significance of seawater intrusion in the Channel decrease as the landward distance away from the sea increases. In addition, seawater intrusion is featured by a distinct annual (369 days) and half-monthly (14.8 days) cycle, corresponding well to annual and half-monthly cycle of tides.
2) The water salinity in the Modaomen channel was significantly and negatively correlated with river discharge. The closer the station is to the channel mouth, the stronger the correlation is, indicating that the suppression of river discharges on seawater intrusion increases downstream. Besides, the salinity of water during seawater intrusion is positively correlated with wind speed.
3) River discharge plays a dominant role in governing seawater intrusion in the Modaomen channel, while wind acts as a minor factor over the long-term temporal scale. River discharges, tides, and wind speed interact and jointly explain 79.4% of the variation of seawater intrusion in the Modaomen channel.

Overall, this study indicates that seawater intrusion in the PRE of China mainly occurs during dry winter periods and has distinctly half-monthly cycle. Because incoming river flow is the dominant factor in affecting seawater intrusion in the Modaomen channel, water resource managers should realize that increasing river discharges, by such as releasing more stored water from upstream-reservoirs to downstream river, is the practical way to prevent inland river seawater intrusion in the PRE. In addition, additional study that considers more influencing factors such as channel bed sand dredging and sea level rise is still needed for helping resource managers and government to better manage seawater intrusion in the PRE of China.

Availability of data and materials The datasets used and analyzed during the current study are available from the corresponding author upon reasonable request.

Declarations

Ethical approval and consent to participate   Not applicable.

Consent for publication   Not applicable.

Competing interests   The authors declare no competing interests.

References

Abd-Elhamid HF, Javadi AA (2011) A density-dependent finite element model for analysis of saltwater intrusion in coastal aquifers. J Hydrol 401(3-4):259–271

Bao Y, Liu J, Ren J, Xu W, Qi Z (2009) Research of law and dynamic mechanism for strong saline water intrusion in Modaomen waterway. Sci China, Ser G 39(10):1527–2534

Chen SS, Fang L, Zhang L, Huang W (2009) Remote sensing of turbidity in seawater intrusion reaches of Pearl River Estuary - a case study in Modaomen water way, China. Estuar Coast Shelf Sci 82(1):119–127

Chen R, Liu C, Gao S (2011) Analysis of the mechanism on the saltwater intrusion in Modaomen estuary. J Hydrodyn 26(03):312–317 (in Chinese)

Chen W, Zou H, Dong Y (2014) Hydrodynamic of saltwater intrusion in the Modaomen waterway (in Chinese). Adv Water Sci 25(05):713–723

Chen YX, Zuo J, Zou H, Zhang M, Zhang K (2016) Responses of estuarine salinity and transport processes to sea level rise in the Zhujiang (Pearl River) Estuary. Acta Oceanol Sin 35(5):38–48

Chen J, Jiang C, Wu Z, Long Y, Deng B, Liu X (2019) numerical investigation of fresh and salt water distribution in the Pearl River Estuary during a typhoon using a fully coupled atmosphere-wave-ocean model. Water 11:646

Cheng XJ, Zhan W, Guo Z, Yuan L (2012) A modeling study on saltwater intrusion to western four watercourses in the Pearl River Estuary. China Ocean Eng 26(4):575–590

Cui WZ, Chen J, Wu YP, Wu YD (2007) An overview of water resources management of the Pear River. Water Sci Technol Water Supply 7(2):101–113

Cui B, Shao X, Zhang Z (2015) Assessment of flow paths and confluences for saltwater intrusion in a deltaic river network. Hydrol Process 29:4549–4558

Fang S (2013) Analysis on main driving factors of saline water intrusion in Modaomen Waterway of Pearl River. Yangtze River 44(05):23–26 (in Chinese)

Franceschini F, Signorini R (2016) Seawater intrusion via surface water vs. deep shoreline salt-wedge: a case history from the Pisa coastal plain (Italy). Groundw Sustain Dev 2-3:73–84

Gain AK, Giupponi C, Renaud FG (2012) Climate change adaptation and vulnerability assessment of water resources systems in developing countries: a generalized framework and a feasibility study in Bangladesh. Water 4:345–366

Gao C, Cai D (2020) Effect mechanism of the north wind on saltwater intrusion in the Modaomen channel. Pearl River 41(2):12–20 (in Chinese)

Garcia A, Juanes JA, Alvarez C, Revilla JA, Medina R (2010) Assessment of the response of a shallow macrotidal estuary to changes in hydrological and wastewater inputs through numerical modelling. Ecol Model 221(8):1194–1208

Gong W, Shen J (2011) The response of salt intrusion to changes in River discharge and tidal mixing during the dry season in the Modaomen Estuary. China Cont Shelf Res 31(2011):769–788

Gong WP, Maa JPY, Hong B, Shen J (2014) Salt transport during a dry season in the Modaomen Estuary, Pearl River Delta, China. Ocean Coast Manag 10:139–150

Gong W, Lin Z, Chen Y, Chen Z, Zhang H (2018) Effects of winds and waves on salt intrusion in the Pearl River estuary. Ocean Sci 14:139–159

Grömping U (2006) Relative importance for linear regression in R: the package relaimpo. J Stat Softw 17(1):1–27

Han Z, Tian X, Liu F (2010) Study on the causes of intensified saline water intrusion into Modaomen Estuary of the Zhujiang River in recent years. J Mar Sci 28(02):52–59 (in Chinese)

He Y, Chen S, Huang R, Chen X (2019) Impact of upstream runoff and tidal level on the chlorinity of an estuary in a river network: a case study of Modaomen estuary in the Pearl River Delta, China. J Hydroinf 21(2):359–370

Hong B, Liu Z, Shen J, Wu H, Gong W, Xu H, Wang D (2020) Potential physical impacts of sea-level rise on the Pearl River Estuary, China. J Mar Syst 201:103245

Hou P., Su B., 2009. The numerical model of predicting the salt intrusion in the Pearl River Delta International Conference on Bioinformatics & Biomedical Engineering. IEEE, 1-4.

Hu X, Mao X (2012) Study on the intrusion law of salt tide in Modaomen channel of Pearl River Estuary. J Hydraul Eng 43(05):529–536 (in Chinese)

Hu J, Liu B, Peng S (2019) Forecasting salinity time series using RF and ELM approaches coupled with decomposition techniques. Stoch Env Res Risk A 33(4-6):1117–1135

Huang R, Chen X, He Y, Yu H (2017) Simulation and analysis of chlorinity of the Modaomen Estuary based on BP neural networks. China Rural Water Hydropower 2017(04):101–105 (in Chinese)

Javadi, A.A., M.S. Hussain, H.F. Abdelhamid, M.M. Sherif, 2013. Numerical modelling and controls of seawater intrusion in coastal aquifers. Proceedings of the 18th international conference on soil mechanics and geotechnical engineering, Paris, 2013, pp, 739-742

Jia LW, Wu CY, Ren J, Lei YP, Zhou SH (2006) Hydrologic characteristics and estuarine dynamic processes during the dry season in Modaomen Estuary of the Pearl River. Adv Water Sci 17(1):82–88 (in Chinese)

Johnson JW, Lebreton JM (2004) History and use of relative importance indices in organizational research. Organ Res Methods 7(3):238–257

Kong L, Chen X, Wen P, Liu B (2011) Analysis on severe saltwater intrusion in Modaomen Channel of the Pearl River estuary in dry season during 2009-2010. J Nat Resour 26(11):1858–1865 (in Chinese)

Kruskal W (1987) Relative importance by averaging over orderings. Am Stat 41:6–10

Lin Z, Zhang H, Lin H, Gong W (2019) Intraseasonal and interannual variabilities of saltwater intrusion during dry seasons and the associated driving forcing in a partially mixed estuary. Cont Shelf Res 174:95–107

Liu Y (2020) Tendency of fluvial process and hydrologic extreme events in river network of Pearl River Delta under changing environment. J China Hydrol 40(3):71–75 (in Chinese)

Liu X, Wei X, Cai B, Yang H (2010) A preliminary analysis of relationships between saline water intrusion and the change of wind at Pearl River Mouth in autumn of 2009. Guangdong Meteorol 32(02):11–13 (in Chinese)

Liu B, Yan S, Chen X, Lian Y, Xin Y (2014) Wavelet analysis of the dynamic characteristics of saltwater intrusion – a case study in the Pearl River Estuary of China. Ocean Coast Manag 95:81–92

Liu B, Huang Y, Liu L, Wen P (2016) Analysis of change characteristics of gate waterway in Pearl River since 2005 a Salty Field. Pearl River 37(05):30–33 (in Chinese)

Liu B, Liao Y, Yan S, Yan H (2017) Dynamic characteristics of saltwater intrusion in the Pearl River Estuary. China Nat Hazards 89(3):1097–1117

Liu B, Peng S, Liao Y, Long W (2018) The causes and impacts of water resources crises in the Pearl River Delta. J Clean Prod 177:413–425

Liu B, Peng S, Liao Y, Wang H (2019a) The characteristics and causes of increasing severe saltwater intrusion in Pearl River Estuary. Estuar Coast Shelf Sci 220:54–63

Liu C, Yu M, Cai H, Chen X (2019b) Recent changes in hydrodynamic characteristics of the Pearl River Delta during the flood period and associated underlying causes. Ocean Coast Manag 179:104814

Liu, C., Yu, M., Jia, L., Cai, H., Chen, X., 2019c. Impacts of physical alterations on salt transport during the dry season in the Modaomen Estuary, Pearl River Delta, China. Estuarine, Coastal Shelf Sci. 227, 106345.

Lu A, Du W (2006) Salty tide tracing back reason in Modaomen Waterway. Guangdong Water Resour Hydropower 2006(05):50–53 (in Chinese)

Mora A, Mahlknecht J, Ledesma-Ruiz R, Sanford WE, Lesser LE (2020) Dynamics of major and trace elements during seawater intrusion in a coastal sedimentary aquifer impacted by anthropogenic activities. J Contam Hydrol 232:103653 (1-17)

Shaha DC, Cho YK, Kim TW (2013) Effects of river discharge and tide driven sea level variation on saltwater intrusion in Sumjin river estuary: an application of finite-volume coastal ocean model. J Coast Res 29(2):460–470

Shi L, Jiao JJ (2014) Seawater intrusion and coastal aquifer management in China: a review. Environ Earth Sci 72(8):2811–2819

Song X, Shi R, Sun L, Xiao H, Long A (2014) Status and cause of saltwater intrusion in Modaomen, Pearl River estuary. Mar Sci Bull 33(01):7–15 (in Chinese)

Sun H, Wang J, Luo W (2012) Measurement of the relative importance of independent variables in linear regression models. Chin J Health Stat 29(6):900–902 (in Chinese)

Tamez-Meléndez C, Hernández-Antonio A, Gaona-Zanella PC, Ornelas-Soto N, Mahlknecht J (2016) Isotope signatures and hydrochemistry as tools in assessing groundwater occurrence and dynamics in a coastal arid aquifer. Environ Earth Sci 75:830. https://doi.org/10.1007/s12665-016-5617-2

Tang G, Yang M, Chen X, Jiang T, Chen T, Chen X, Fang H (2020) A new idea for predicting and managing seawater intrusion in coastal channels of the Pearl River, China. J Hydrol 590:125454. https://doi.org/10.1016/j.jhydrol.2020.125454

Torres-Martinez JA, Mora A, Ramos-Leal JA, Morán-Ramírez J, Mahlknecht J (2019) Constraining a density-dependent flow model with the transient electromagnetic method in a coastal aquifer in Mexico to assess seawater intrusion. Hydrogeol J 27:2955–2972

Twigt D, Goede EDD, Zijl F, Schwanenberg D, Chiu AYW (2009) Coupled 1D-3D hydrodynamic modelling, with application to the Pearl River Delta. Ocean Dyn 59(6):1077–1093

van den Brink M, Huismans Y, Blaas M, Zwolsman G (2019) Climate change induced salinization of drinking water inlets along a tidal branch of the Rhine River: impact assessment and an adaptive strategy for water resources management. Climate 7(4):49

Wang B, Zhu J, Wu H, Yu F, Song X (2012) Dynamics of saltwater intrusion in the Modaomen waterway of the Pearl River Estuary. Sci China-Earth Sci 55(11):1901–1918

Wang H, Li WS, Zuo CS, Dong JX, Li C, Xu H, Liu QL, Pan S (2020) Saltwater intrusion in the Pearl River Estuary (China): variation characteristics and cause analysis[J]. J Coast Res 36:1145–1153

Werner AD, Gallagher MR (2006) Characterization of seawater intrusion in the Pioneer Valley, Australia using hydrochemistry and three-dimensional numerical modelling. Hydrol J 14(8):1452–1469

Wu CD, Hu CX, Zhang JY, Hu B, Wang L, Liang JL (2013) Survey of seawater intrusion in the Pearl River Basin and modeling bromate formation during zonation of the raw water. Ozone Sci Eng 35(6):465–471

Xu Y, Hoitink AJF, Zheng J, Kästner K, Zhang W (2019) Analytical model captures intratidal variation in salinity in a convergent, well-mixed estuary. Hydrol Earth Syst Sci 23(10):4309–4322

You D, Tang C, Deng S, Yang H, Shen D (2009) The characteristics of sea level change around the Pearl River Estuary in recent 15 years and the related severe saline water intrusion. Guangdong Meteorol 31(03):4–5 (in Chinese)

Yuan R, Zhu JR (2015) The effects of dredging on tidal range and saltwater intrusion in the Pearl River Estuary. J Coast Res 31(6):1357–1362

Yuan R, Zhu J, Wang B (2015) Impact of sea-level rise on saltwater intrusion in the Pearl River Estuary. J Coast Res 31(2):477–487

Zhang W, Ruan X, Zheng J, Zhu Y, Wu H (2010) Long-term change in tidal dynamics and its cause in the Pearl River Delta, China. Geomorphology 120(3-4):209–223

Zhang ML, Cui B, Zhang Z, Jiang X (2017) Salinity-oriented environmental flows for keystone species in the Modaomen Estuary, China. Front Earth Sci 11(4):670–681

Zhou X, Yang T, Shi P, Yu Z, Wang X, Li Z (2017) Prospective scenarios of the saltwater intrusion in an estuary under climate change context using Bayesian neural networks. Stoch Env Res Risk A 31(4):981–991

Zou H, Yang F, Zhang L (2019) Effect of riverbed degradation on saltwater intrusion in the Modaomen river channel. Water Resour Power 37(6):36–39 (in Chinese)